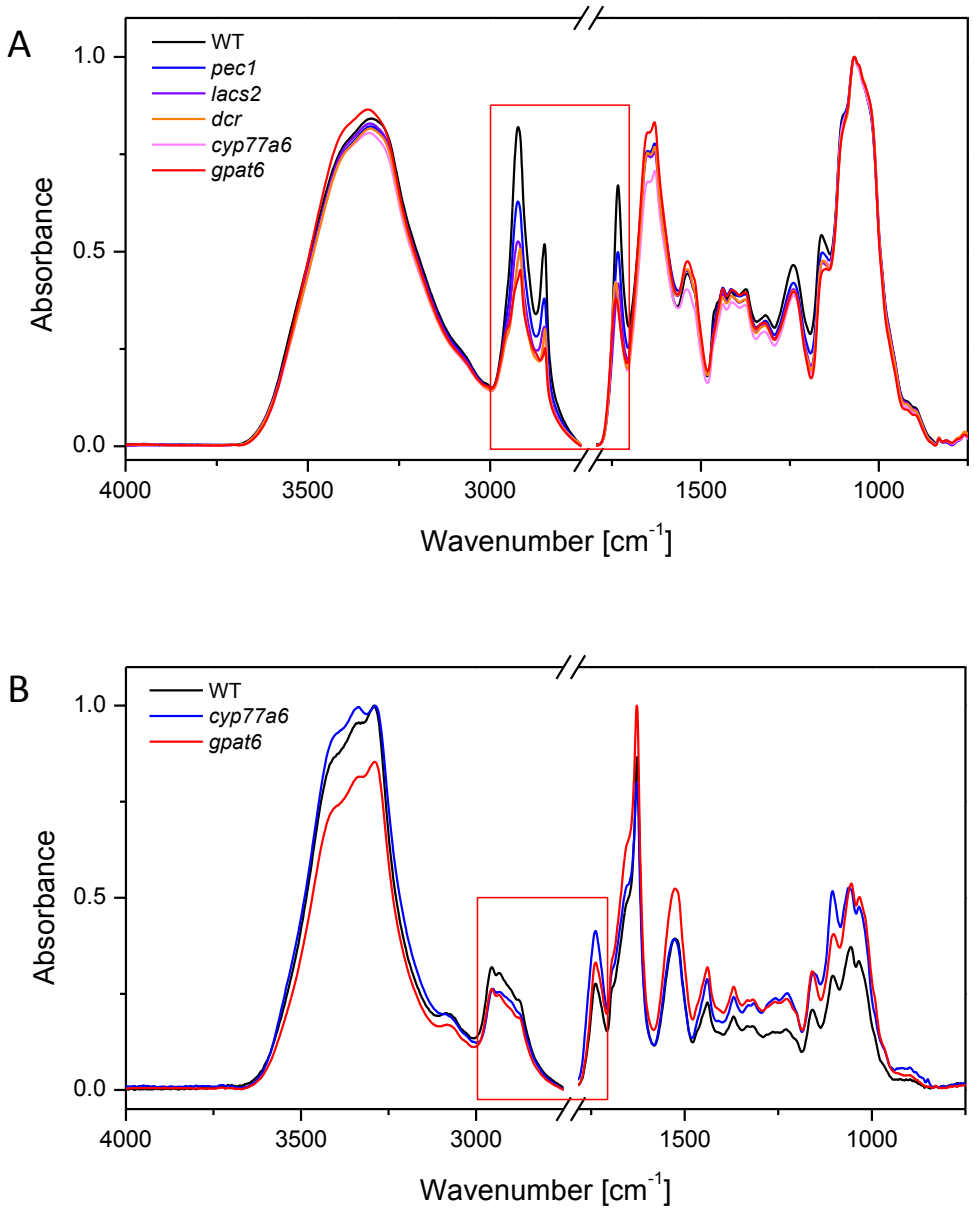

Figure S1 Spectral features of petals of different Arabidopsis genotypes

FTIR spectrotypes showing the entire spectral range are given in (A). The spectral regions of ν(C-H) and ν(C=O) band vibrations that are shown as enlargement in Figure 1 are indicated by a red box. Average FTIR spectra of petals after acid catalyzed depolymerization of polyesters are given in (B). The strong reduction of ν(C-H) and ν(C=O) band vibrations indicates that aliphatic polyesters have been removed. Ester bound decorations of polymers that have not been degraded by this treatment, such as pectin, have been converted to methyl esters, thus indicating the peak position of pectin methyl esterification.

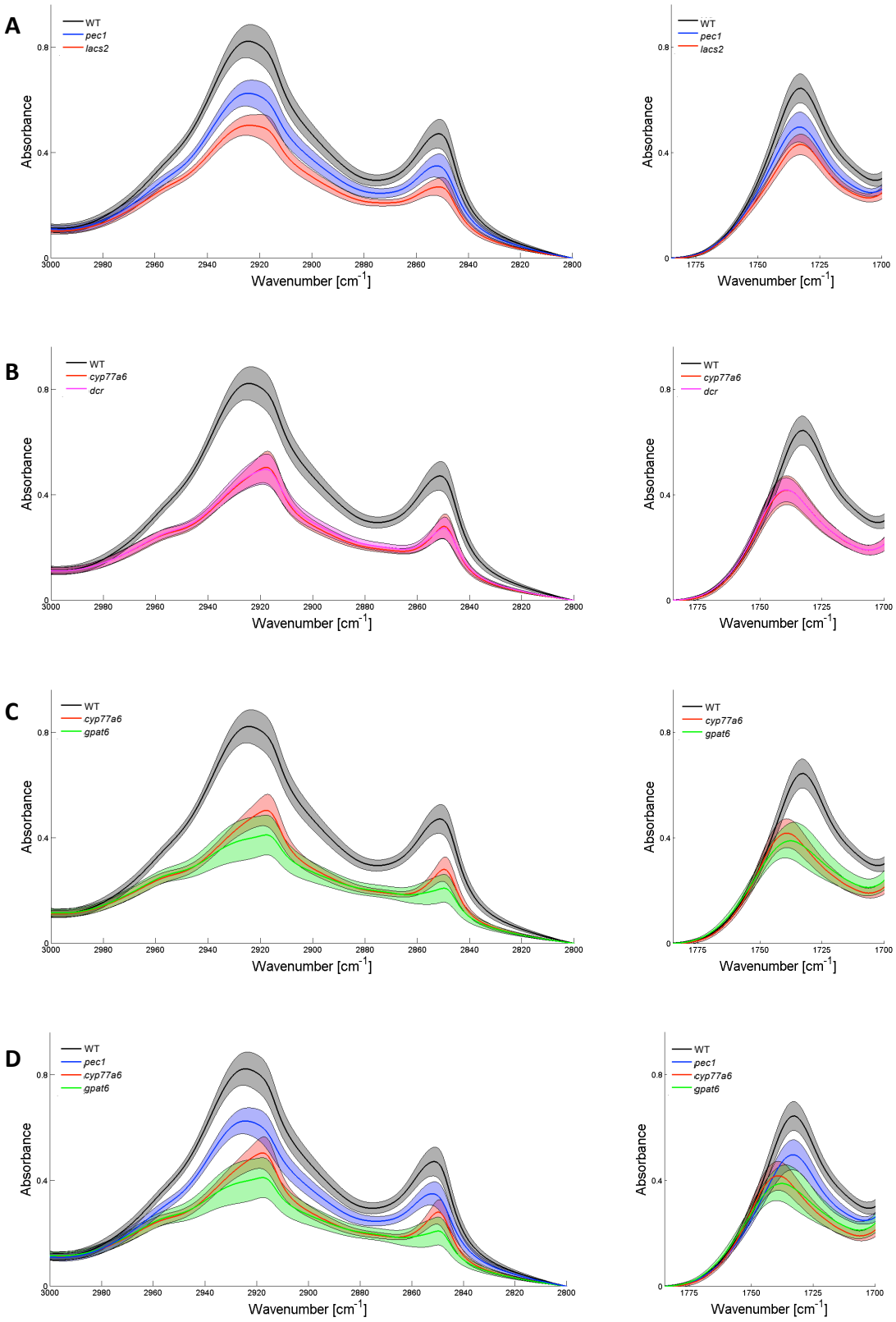

Figure S2 Classification of Arabidopsis cutin mutants by spectrotype

Fragments of FTIR spectrotypes (solid lines) in the ν(C-H) and ν(C=O) vibration regions ±SD of signal intensity (shadows) are shown. Overlay of the spectrotypes of cutin of group (i) plants (WT, *lacs2*, *pec1*) (A), of group (ii) plants (*cyp77a6* and *dcr*) (B), with c*yp77a6* and *gpat6* (C) and with these of *pec1*, *cyp77a6* and *gpat6* (D) identifying three different types of cutin in Arabidopsis petals.

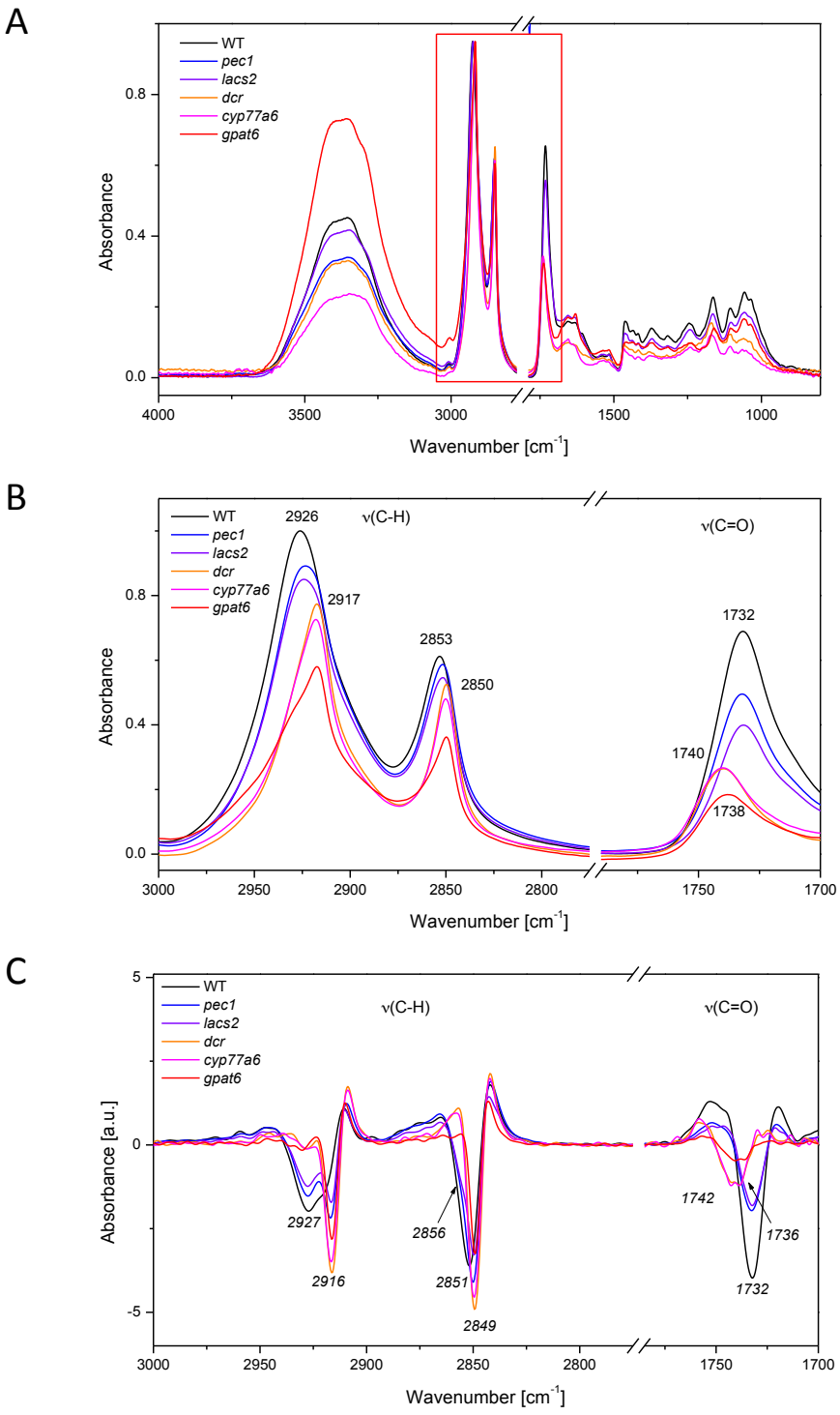

Figure S3 **Spectral features of petals of different genotypes treated with proteinase K and pectolyase**

(A) FTIR spectra over the entire spectral region, (B) enlargement of the regions of ν(C-H) and ν(C=O) band vibrations indicated by a red box in (A), (C) the corresponding 2nd derivatives of the spectra shown in (B). Spectra are scaled arbitrarily for clarity. Numbers indicate positions of peak maxima, numbers in italics indicate contributions revealed by spectra derivatization.

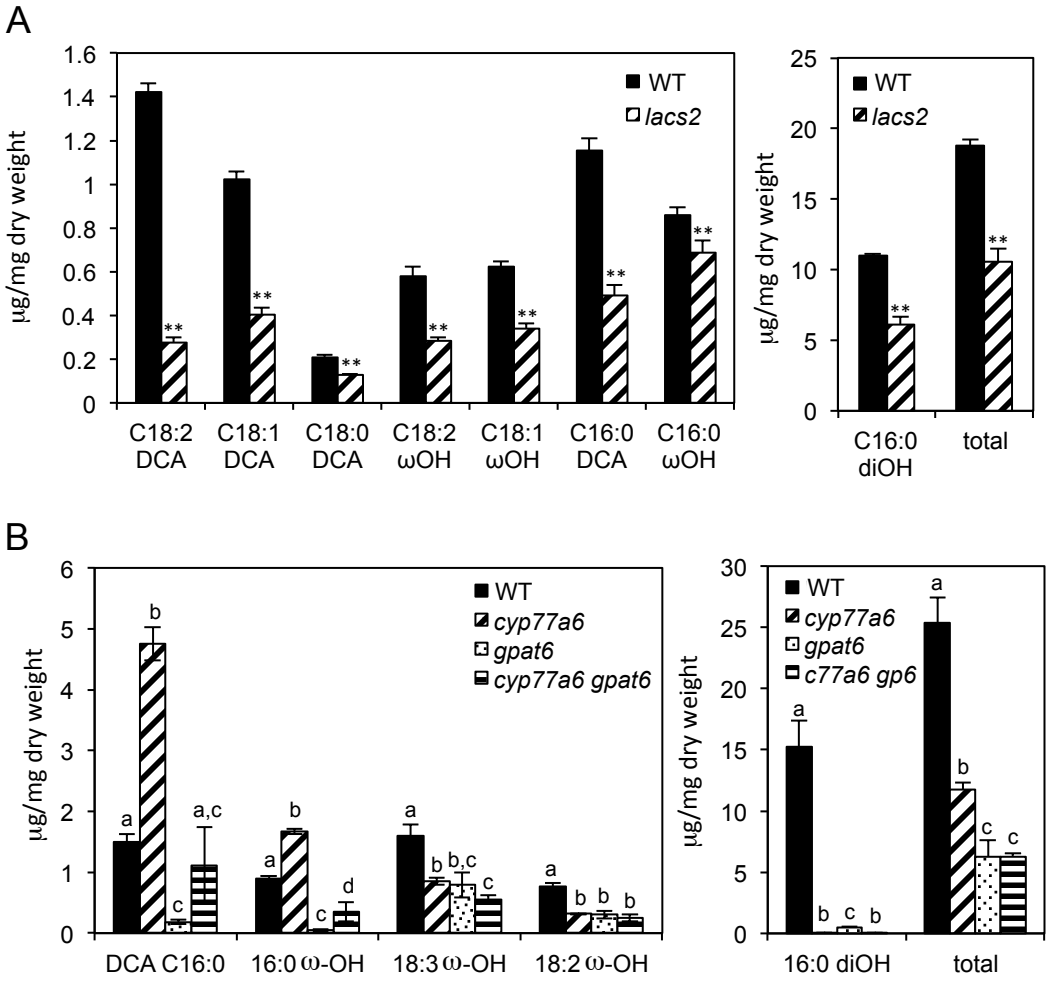

Figure S4 Cutin monomer of petals of *lacs2* and *cyp77a6 gpat6* in comparison to respective controls

Quantification of cutin monomers entire flowers. The graph on the left shows the minor monomers and the one of the right the major monomer 10, 16 diOH C16:0 (C16:0 diOH) and the amount of all analysed monomers (total). ** denote significant differences as determined by students t-test, $p<0.01$. Different lower case letters denote significant differences as determined by ANOVA and post-hoc Tukey HSD test, $p<0.01$.

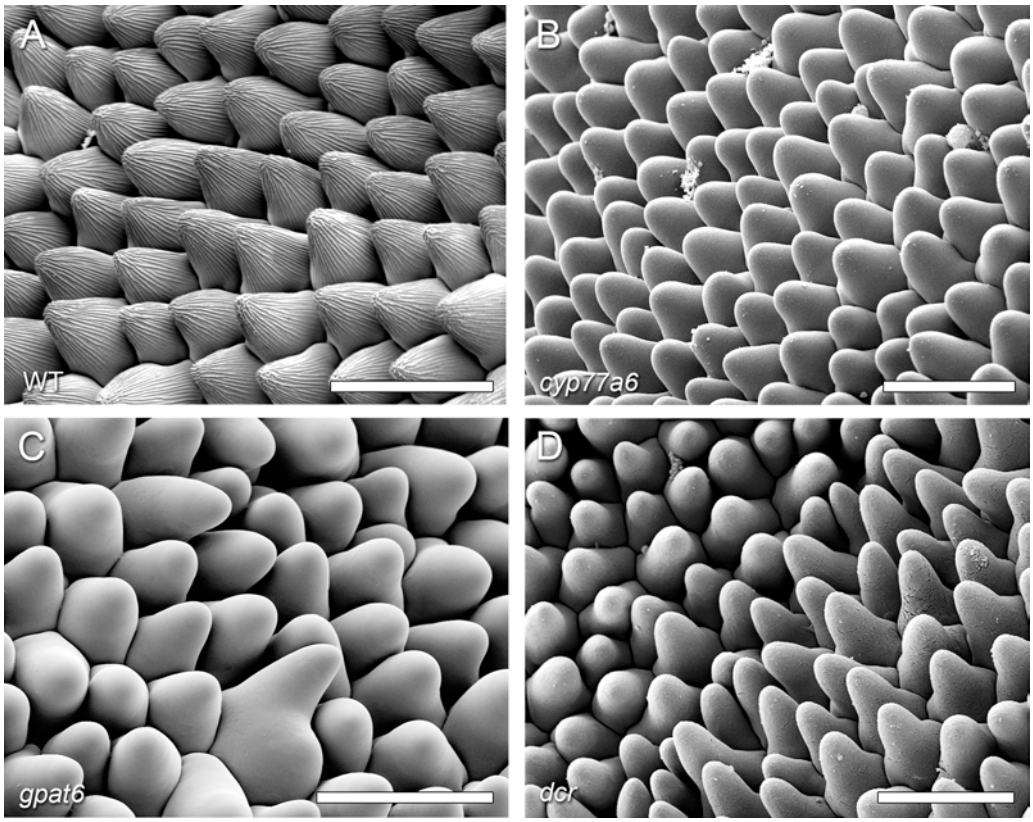

Figure S5 Shape and surface structure of epidermal cells on the adaxial side of the petal of Arabidopsis genotypes having a strongly reduced amount of 10, 16 diOH C16:0

In contrast to the WT having typical nanoridges, *cyp77a6*, *gpat6* and *dcr* have no nanoridges on their surface. While epidermal cells of *cyp77a6* and *gpat6* are more roundish than WT epidermal cells, these of *dcr* are more pointy and elongated. Cryo-fixed flowers were depicted on the upper third of the petal blade. Scale bars represent 30 µm.

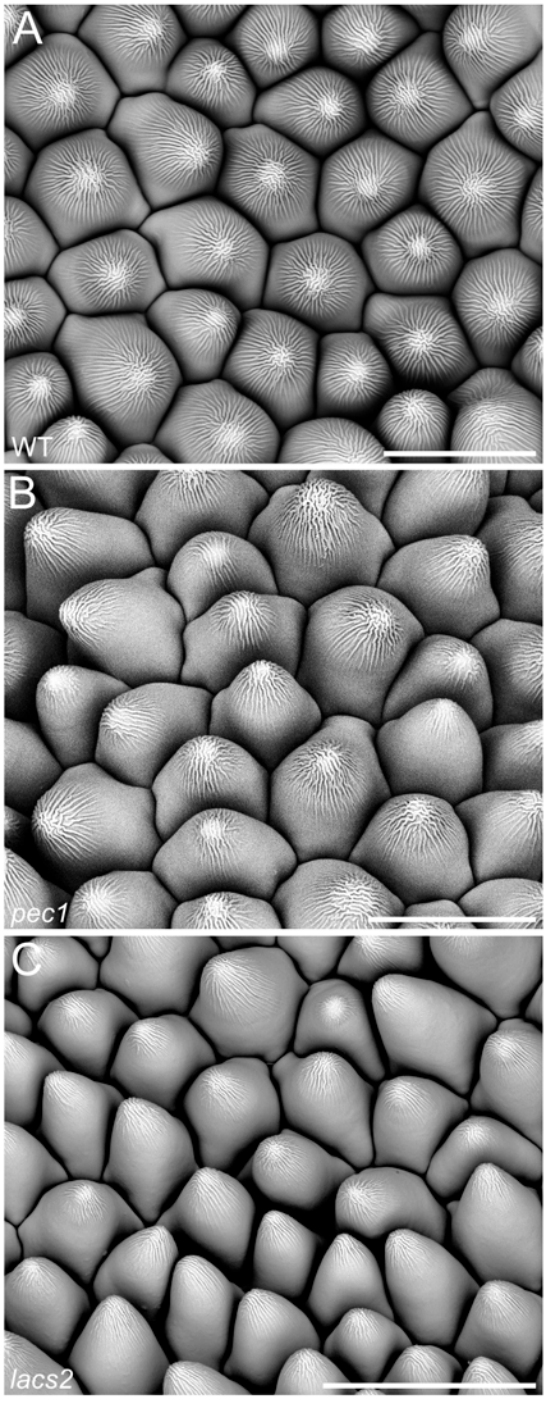

Figure S6 Shape and surface structure of epidermal cells on the adaxial side of the petal of Arabidopsis genotypes having reduced amounts of cutin

In contrast to the WT having deep nanoridges, *pec1* and *lacs2* have modified nanoridge formation on the surface of epidermal cells. While epidermal cells of *pec1* have a sligtly more roundish shape than WT epidermal cells, these of *lacs2* are more irregular and often pointy. Cryo-fixed flowers were depicted on the upper third of the petal blade. Scale bars represent 20 µm in A and B and 30 µm in C.

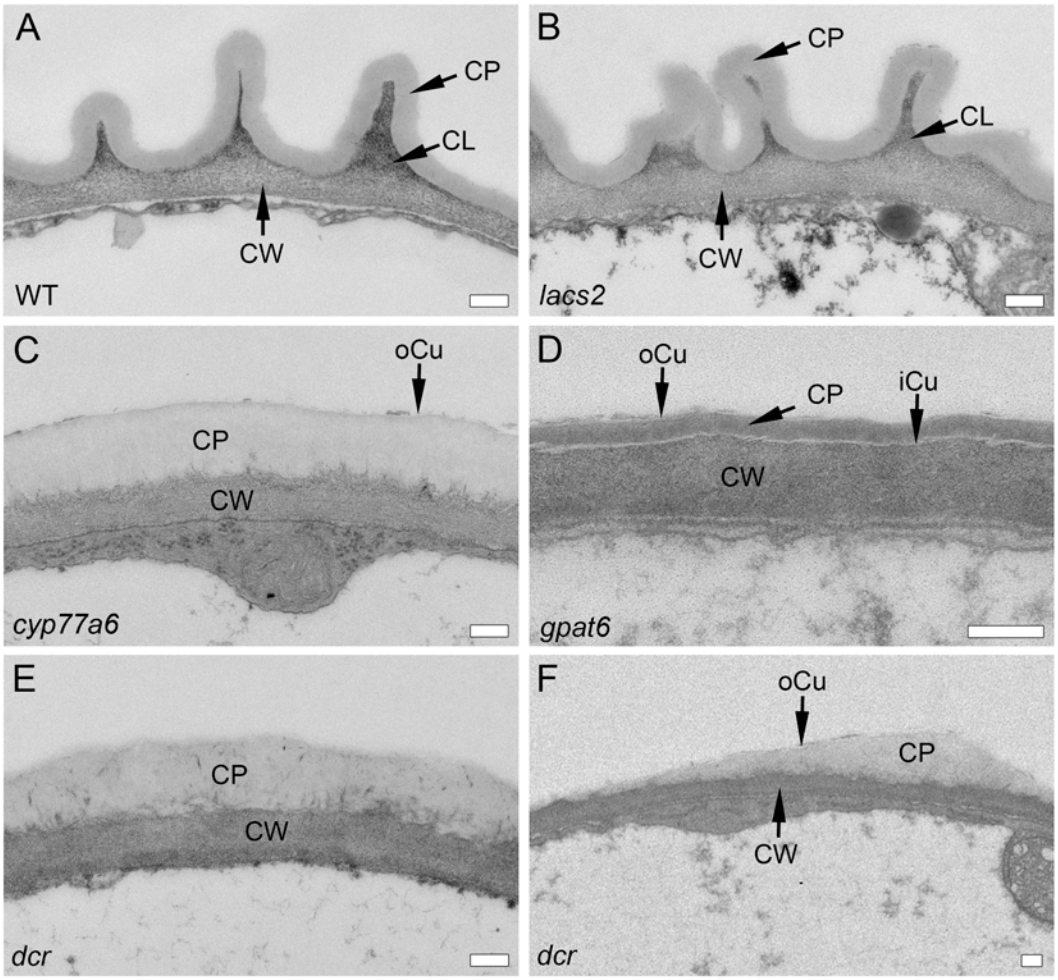

Figure S7 Cuticle ultrastructure on the abaxial side of petals in different genotypes of Arabidopsis

The cellwall-cuticle continuum was depicted at the apex of the conical epidermal cell of petals that were embedded in Spurr resin. CL, cuticular layer; Cu, cuticle; iCu, inner cuticle; oCu, outer cuticle; CP, cuticle proper; CW, cell wall; Scale bars represent 200 nm.

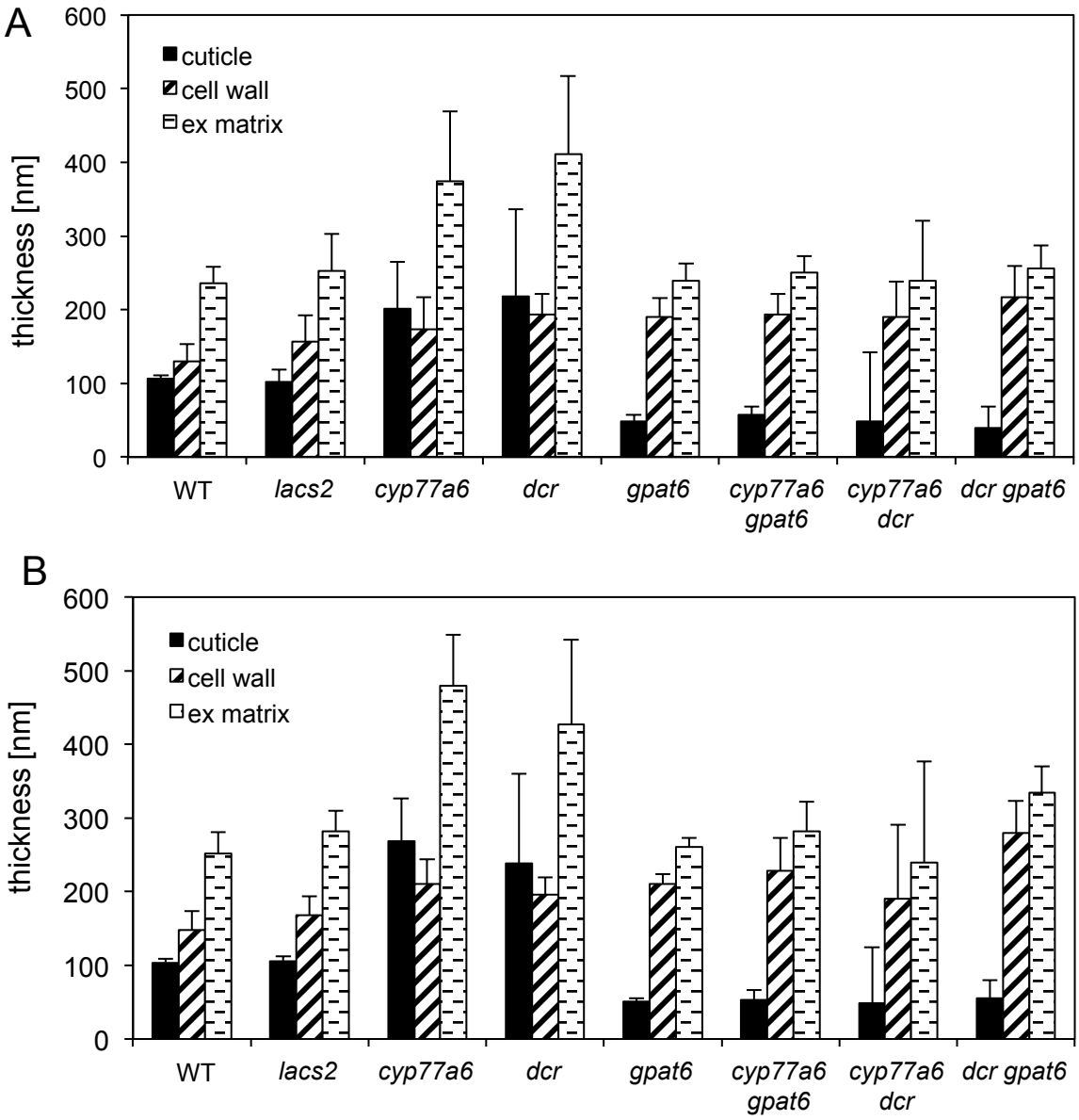

Figure S8 **Dimensions of the extracelluar matrix of petal epidermal cells in different Arabidopsis genotypes**

The dimensions of the cuticle and cell wall was measured at the top of the epidermal cell on the adaxial (A) and abaxial (B) side of the petal. The WT and *lacs2* cuticle was measured in between the nanoridges. Three different areas in 6 - 7 TEM pictures were evaluated. Ex matrix, entire extracellular matrix. The measurements were repeated once with similar results.

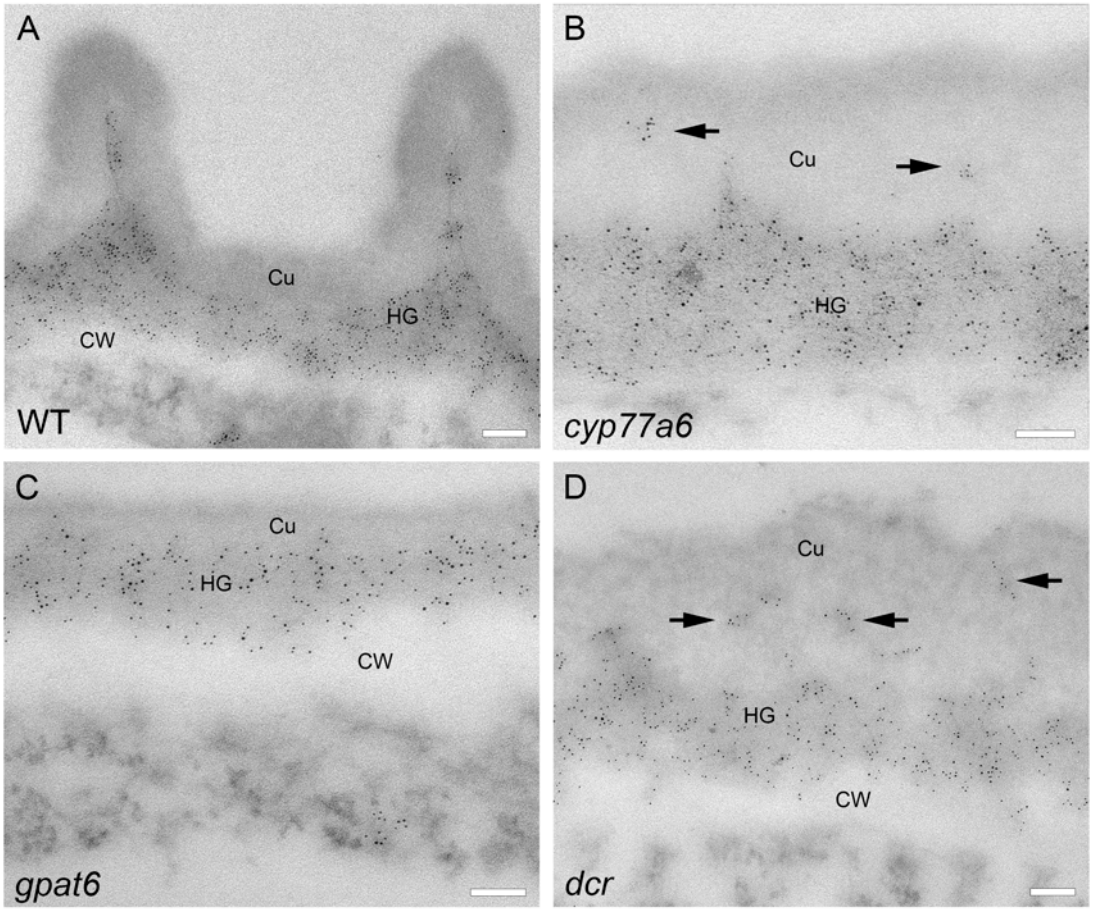

Figure S9 **Localization of homogalacturonan in the cell wall-cuticle continuum on the abaxial side of petals of different Arabidopsis genotypes**

LM20-labeling of esterified homogalacturonan domains (HG) on sections embedded in LR-white resin. The cell wall-cuticle continuum was depicted at the apex of petal epidermal cell. Cu, cuticle, CW, cell wall. Black arrows point to dispersed LM20-labeled material. Scale bars represent 100 nm.

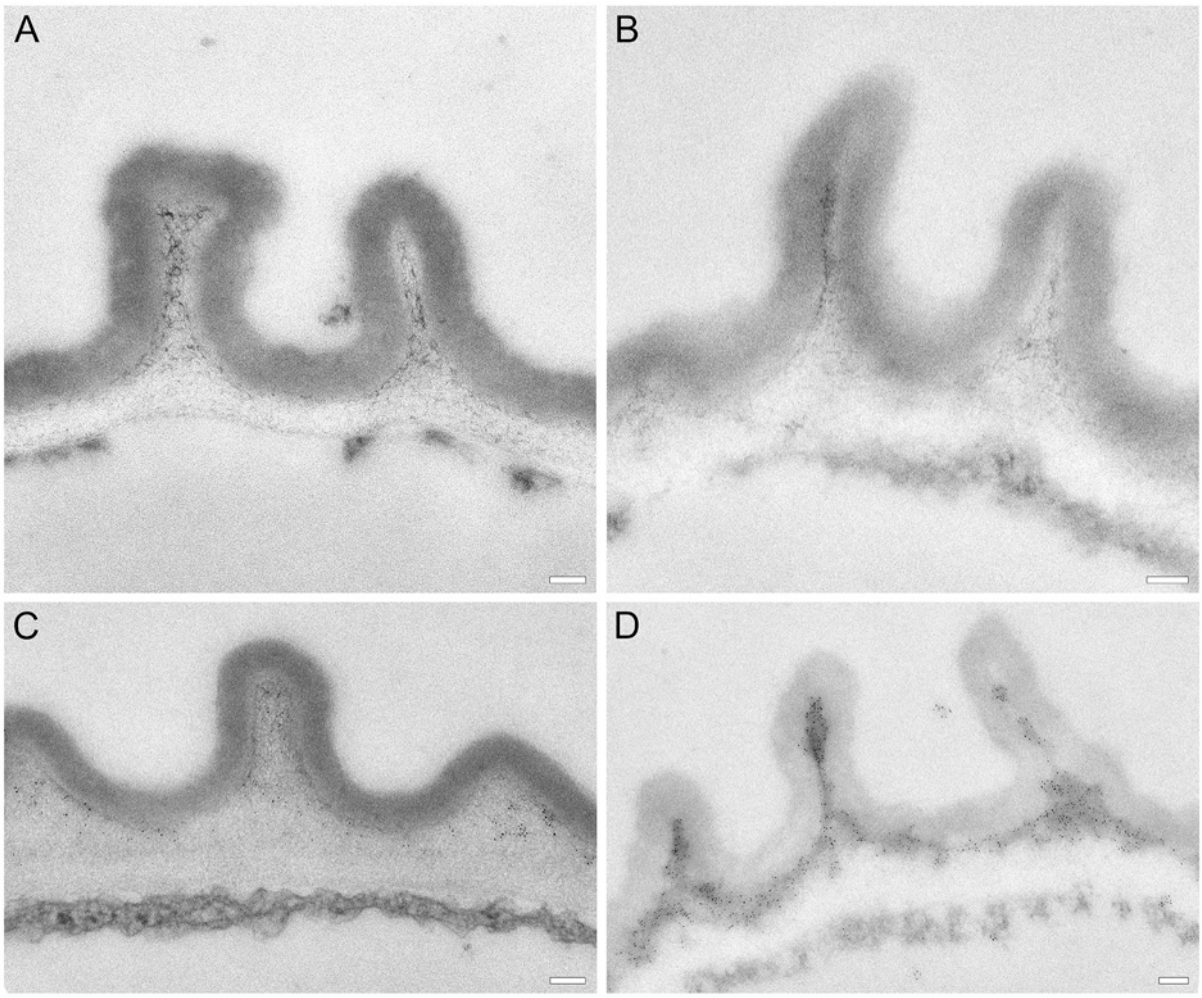

Figure S10 **Immunogold-labeling controls of epidermal petal cells of Arabidopsis wildtype**

Immunogold-labeling procedure on sections prepared for immunocytochemistry without primary antibody in (A) and on sections prepared for immunocytochemistry without secondary antibody in (B). Labeling of homogalacturonan (HG) with LM20 on sections prepared for ultrastructural analyses in (C). Labeling of HG with LM19 on sections prepared for immunocytochemistry in (D). Scale bars represent 100 nm.